Active Site of Chondroitin AC Lyase Revealed by the Structure of Enzyme−Oligosaccharide Complexes and Mutagenesis[†,‡]

Weijun Huang,[§] Lorena Boju,[§] Lydia Tkalec,[||,⊥] Hongsheng Su,[||,#] Hyun-Ok Yang,[▽] Nur Sibel Gunay,[▽] Robert J. Linhardt,[▽] Yeong Shik Kim,[○] Allan Matte,[§] and Miroslaw Cygler*[,§]

Biotechnology Research Institute, 6100 Royalmount Avenue, Montréal, Québec H4P 2R2 Canada, Montreal Joint Centre for Structural Biology, Montréal, Québec, Canada, IBEX Technologies Inc., 5485 Pare Street, Montréal, Québec H4P 1P7 Canada, Department of Chemistry, Division of Medicinal Chemistry and Department of Chemical and Biochemical Engineering, The University of Iowa, 115 South Grand Avenue, PHAR S328, Iowa City, Iowa 52242-1112, and Natural Products Research Institute, Seoul National University, Seoul 110-460, Korea

Received October 17, 2000; Revised Manuscript Received December 18, 2000

ABSTRACT: The crystal structures of *Flavobacterium heparinium* chondroitin AC lyase (chondroitinase AC; EC 4.2.2.5) bound to dermatan sulfate hexasaccharide (DS^{hexa}), tetrasaccharide (DS^{tetra}), and hyaluronic acid tetrasaccharide (HA^{tetra}) have been refined at 2.0, 2.0, and 2.1 Å resolution, respectively. The structure of the Tyr234Phe mutant of AC lyase bound to a chondroitin sulfate tetrasaccharide (CS^{tetra}) has also been determined to 2.3 Å resolution. For each of these complexes, four (DS^{hexa} and CS^{tetra}) or two (DS^{tetra} and HA^{tetra}) ordered sugars are visible in electron density maps. The lyase AC DS^{hexa} and CS^{tetra} complexes reveal binding at four subsites, −2, −1, +1, and +2, within a narrow and shallow protein channel. We suggest that subsites −2 and −1 together represent the substrate recognition area, +1 is the catalytic subsite and +1 and +2 together represent the product release area. The putative catalytic site is located between the substrate recognition area and the product release area, carrying out catalysis at the +1 subsite. Four residues near the catalytic site, His225, Tyr234, Arg288, and Glu371 together form a catalytic tetrad. The mutations His225Ala, Tyr234Phe, Arg288Ala, and Arg292Ala, revealed residual activity for only the Arg292Ala mutant. Structural data indicate that Arg292 is primarily involved in recognition of the *N*-acetyl and sulfate moieties of galactosamine, but does not participate directly in catalysis. Candidates for the general base, removing the proton attached to C-5 of the glucuronic acid at the +1 subsite, are Tyr234, which could be transiently deprotonated during catalysis, or His225. Tyrosine 234 is a candidate to protonate the leaving group. Arginine 288 likely contributes to charge neutralization and stabilization of the enolate anion intermediate during catalysis.

Glycosaminoglycans (GAGs)[1] are highly negatively charged polysaccharides, formed from disaccharide repeating units. Each unit contains *N*-acetylated or *N*-sulfonated and usually *O*-sulfonated D-galactosamine (chondroitin and dermatan sulfates) and D-glucosamine (heparin, heparan sulfate, keratan sulfate, and hyaluronan) attached through β- or α-(1,4) linkages to D-glucuronic or L-iduronic acid (heparin, heparan sulfate, chondroitin sulfate, dermatan sulfate and hyaluronan) or through a β-(1,3) linkage to D-galactose (keratan sulfate). These disaccharides are linked in turn by α- or β-(1,3 or 1,4) linkages forming the polysaccharide chain (Figure 1) (*1*). The negative charge of these polymers is due to extensive N-2, O-3, or O-6 sulfonation of D-glucosamine or O-4 and O-6 sulfonation of *N*-acetyl-D-galactosamine. In addition, these polysaccharides contain a carboxylate moiety and possible O-2 sulfonation of their uronic acid units. Glycosaminoglycans, with the exception of hyaluronan, are attached to a protein core and form a proteoglycan, the main component of the extracellular matrix (*2*). A number of bacterial species, including *Flavobacterium heparinum* syn-

[†] This work was supported in part by a NRC/NSERC Partnership Program Grant from the Natural Sciences and Engineering Research Council of Canada (M.C.) and grants HL52622 and GM38060 from the National Institutes of Health (R.J.L.).

[‡] The models have been deposited in the Protein Data Bank with access codes 1HM2, 1HMU, 1HM3, and 1HMW for the lyase AC-DS^{hexa}, -DS^{tetra}, -HA^{tetra} and -CS^{tetra} complexes, respectively.

* To whom correspondence should be addressed. Phone: (514) 496-6321. Fax: (514) 496-5143. E-mail: mirek.cygler@bri.nrc.ca.

[§] Biotechnology Research Institute and Montreal Joint Centre for Structural Biology.

[||] IBEX Technologies Inc.

[⊥] Present Address: Merck-Frost Research Laboratories, Kirkland, Québec, Canada.

[#] Present Address: Theratechnologies Inc. 2310 Boulevard Alfred-Nobel, Saint-Laurent, Quebec, Canada H4S 2A4.

[▽] Department of Chemistry.

[○] Natural Products Research Institute.

[1] Abbreviations: AUFS, absorbance units full scale; CE, capillary electrophoresis; GalNAc, *N*-acetyl-galactosamine; GlcNAc, *N*-acetyl-glucosamine; EDTA, ethylenediamine tetraacetic acid; ESI-MS, electrospray ionization mass spectrometry; FPLC, fast protein liquid chromatography; GlcUA, glucuronic acid; IdoUA, iduronic acid; GAG, glycosaminoglycan; ABC I lyase, chondroitin sulfate ABC lyase I from *Proteus vulgaris*; ABC II lyase, chondroitin sulfate ABC lyase II from *Proteus vulgaris*; lyase AC, Chondroitin lyase AC from *Flavobacterium heparinum*; CS^{tetra}, chondroitin sulfate tetrasaccharide; DS^{hexa}, dermatan sulfate hexasaccharide; DS^{tetra}, dermatan sulfate tetrasaccharide; HA^{tetra}, hyaluronic acid tetrasaccharide; PMSF, phenylmethanesulfonyl flouride; SAX-HPLC, strong anion exchange−high performance liquid chromatography.

10.1021/bi0024254 CCC: $20.00
Published on Web 01/31/2001

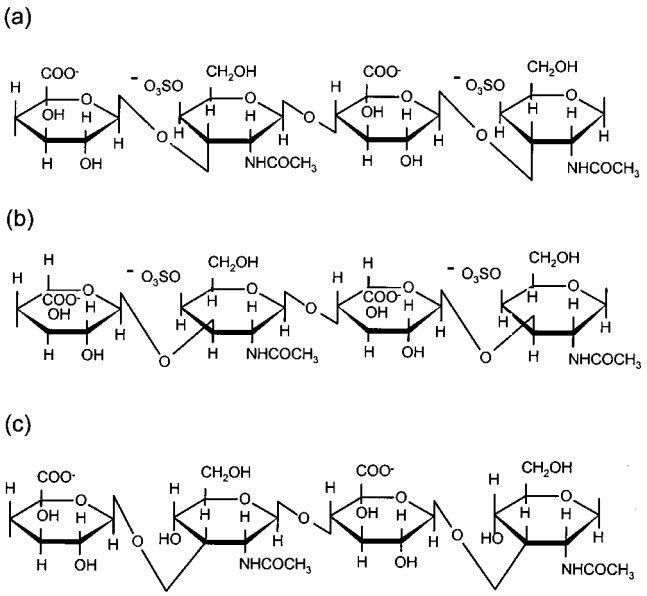

FIGURE 1: Structures of GAG tetrasaccharides: (a) chondroitin-4-sulfate, (b) dermatan-4-sulfate, (c) hyaluronic acid (hyaluronan). Each disaccharide consists of L-iduronic acid linked α(1,3) (dermatan sulfate) or D-glucuronic acid linked β(1,3) (chondroitin sulfate) to 2-deoxy-2-acetamido-D-galactose (dermatan and chondroitin sulfates) or 2-deoxy-2-acetamido-D-glucose (hyaluronic acid). Successive disaccharide units are attached by a β(1,4) linkage.

thesize GAG lyases, enzymes used to degrade and utilize glycosaminoglycans as a source of carbon in the bacterium's natural environment (*3*, *4*).

Degradation of glycosaminoglycans occurs via two possible mechanisms: hydrolysis and lytic β-elimination, with the exception of keratan sulfate which can only be degraded hydrolytically (reviewed in refs *3* and *5*). Polysaccharide hydrolases are presently better understood than the lyases, and their reaction mechanism is well characterized. The lyases have been characterized as to their substrate specificity and mode of action (*7*−*9*), but the reaction mechanism at the molecular level is poorly understood. Lyases cleave the (1,4) bond on the nonreducing end of the uronic acid, yielding an unsaturated product. A chemically plausible mechanism for the β elimination reaction has been proposed (*10*), yet its details in the enzyme setting have not been fully confirmed. On the basis of the structures of enzyme−substrate or product complexes and site-specific mutagenesis, mechanisms have been recently proposed for pectate lyases C (*11*) and B (*12*), chondroitinase B (*13*), and two hyaluronate lyases (*14*−*16*), however, they require further validation.

In topological terms, the known structures of polysaccharide lyases fall within two protein fold families. Pectin and pectate lyases (reviewed in ref *12*), as well as chondroitin lyase B (*13*) belong to the right-handed parallel β-helix family and have the substrate-binding site in roughly the same topological location. This topological family contains not only polysaccharide lyases but also polysaccharide hydrolases (*12*, *17*). Chondroitinase B (*13*) is the only GAG lyase that belongs to this family. The second topological family, all of which contain a domain consisting of an incomplete $(\alpha/\alpha)_5$ toroid, includes chondroitin AC lyase (*18*), *Streptococcus pneumoniae* hyaluronate lyase (*14*), and alginate lyase A1-III from *Sphingomonas* species A1 (*19*).

The mode of action of chondroitinase AC (hereafter lyase AC; EC 4.2.2.5) has been established as random endolytic (*7*, *9*, *20*). It degrades chondroitin, chondroitin 4-sulfate, chondroitin 6-sulfate, as well as hyaluronic acid. Dermatan sulfate differs from chondroitin sulfate only in that in place of D-glucuronic acid it contains its C-5 epimer, L-iduronic acid. It has been demonstrated that *F. heparinum* lyase AC can cleave dermatan sulfate *only* at (1−4) linkages where D-glucuronic acid and not L-iduronic acid is located at the reducing end of the cleavage site and inhibits the enzyme with a $K_I \approx 0.2$ μM (*21*).

A number of bacterial hyaluronate lyases share significant sequence homology to *F. heparinum* lyase AC, having between 16% and 22% overall sequence identity (*18*). Many of the identical residues conserved in the sequence alignment are found to map to a long cleft in *F. heparinum* lyase AC, with several of these suggested to play a role in either substrate binding or catalysis (*14*−*16*, *18*).

To identify more directly residues involved in the catalysis of lyase AC we have prepared crystals of complexes of the enzyme with three oligosaccharides: dermatan sulfate hexasaccharide, dermatan sulfate tetrasaccharide and hyaluronic acid tetrasaccharide. On the basis of our earlier analysis (*18*) and the structures of the lyase AC-oligosaccharide complexes described herein we have selected His225, Tyr234, Arg288, and Arg292 as the most likely candidates for the active site residues and mutagenized each of these four positions. We have also cocrystallized one of these mutant enzymes, lyase AC Tyr234Phe, with a chondroitin sulfate tetrasaccharide. Combined, these studies yield new insights into the catalytic machinery and possible mechanisms for lyase AC.

MATERIALS AND METHODS

Materials. Chondroitin-4-sulfate from bovine trachea, chondroitin-6-sulfate from shark cartilage and heparin sulfate from bovine intestinal mucosa were purchased from Fluka (Oakville, ON, Canada). Semi-purified heparin (sodium salt) and dermatan sulfate from porcine intestinal mucosa (MW_{avg}, 40 000) were obtained from Celsus Laboratories, Cincinnati, OH. Hyaluronan (MW_{avg}, 100 000) from *Streptococcus Zooepidemicus* was obtained from Kibun Food Chemipla Co. (Tokyo, Japan). Chondroitin 4-sulfate (for preparation of oligosaccharides; MW_{avg} 25 000) chondroitin ABC lyase (EC 4.2.2.4) and hyaluronidase (EC 3.2.1.35) were from Sigma Chemical Co. (St. Louis, MO). Gel permeation chromatography was performed on Bio-Gel P2, P6 (superfine) and P10 (superfine) from Bio-Rad (Richmond, CA) or Sephadex G10 and G50 (superfine) from Pharmacia. SP−Sepharose Big Beads (100−300 μm) Bioprocess media was from Pharmacia, Ceramic hydroxyapatite (20 μm bead diameter) was from American International Chemical Inc. (Natick, MA). Complete EDTA-free protease inhibitor cocktail tablets, as well as individual protease inhibitors, were obtained from Roche Diagnostics (Laval, Quebec). All DNA-modifying and restriction enzymes were purchased from either Amersham-Pharmacia or New-England Biolabs (Beverly, Massachusetts) and used according to the manufacturer's recommendations. All other reagents used were of analytical grade.

Preparation of Dermatan Sulfate, Chondroitin Sulfate, and Hyaluronic Acid Oligosaccharides. (i) Enzymatic Depolymerization of Glycosaminoglycans. Dermatan sulfate (500 mL,

20 mg/mL) in 50 mM Tris HCl-sodium acetate buffer, pH 8.0 was treated with chondroitin ABC lyase (20 units) at 37 °C. When the absorbance at 232 nm indicated the digestion was 50% completed, the digestion mixture was heated at 100 °C for 3 min and concentrated by rotary evaporation to 100 mL for fractionation by low-pressure GPC.

Chondroitin 4-sulfate (5 g dissolved in 100 mL 50 mM sodium phosphate buffer) was treated with 5 units of chondroitin ABC lyase at 37 °C and the reaction was terminated at 55% completion by boiling for 5 min and the reaction mixture freeze-dried.

Hyaluronic acid, 500 mg dissolved in 30 mL of 0.1 M sodium phosphate buffer at pH 5.0, was treated with 100 mg of hyaluronidase (750−1500 units/mg of solid). During the incubation for 48 h at 37 °C, an additional 100 mg of enzyme was added at the end of each 12 h interval. The solution was boiled for 3 min to stop the reaction and was freeze-dried.

(ii) Purification of Oligosaccharides. A portion (1.25 g in 12.5 mL) of the dermatan and chondroitin sulfate oligosaccharide mixtures were fractionated into disaccharide through dodecasaccharide components on a Bio-Gel P6 column (4.8 × 100 cm) or Bio-Gel P10 column (2.5 × 110 cm) eluted with 100 mM sodium chloride at a flow rate of 1.5 mL/min, with absorbance detection at 232 nm. Fractions consisting of tetrasaccharides and hexasaccharides, were concentrated by rotary evaporation. The tetrasaccharide and hexasaccharide fractions were desalted by GPC on a Bio-Gel P2 or a Sephadex G-10 column, concentrated again and freeze-dried.

Charge separation of the tetrasaccharide and hexasaccharide mixtures was carried out by semipreparative SAX-HPLC on 5 μm Spherisorb columns of dimensions 2.0 × 25 cm and 0.46 × 25 cm from Waters (Milford, MA) using a linear (0 to 2 M) gradient of sodium chloride at pH 3.5. HPLC was performed on a Shimadzu 10A*i* chromatography system (Kyoto, Japan). The major peaks obtained from each sized mixture were pooled, lyophilized, and desalted on a Bio-Gel P2 column. Each peak was next analyzed by analytical SAX-HPLC and CE. CE was performed using a ISCO Capillary Electrophoresis system on a fused silica capillary, 50 μm i.d., 360 μm o.d., 62 cm in long, 42 cm effective length, from ISCO, Inc. (Nebraska, NE). The hyaluronan oligosaccharide mixtures were similarly fractionated over a Sephadex G-50 column and eluted with water. Carbazole (uronic acid) assay was performed for each tube and the absorbance at 525 nm was measured. The major tetrasaccharide product was collected and concentrated by freeze-drying.

The purity of the tetrasaccharides and hexasaccharide was monitored by CE and analytical SAX-HPLC. CE was performed on a fused silica capillary in the reverse polarity mode. The sample was applied at the cathode and eluted with 20 mM phosphoric acid adjusted to pH 3.5 with saturated dibasic sodium phosphate (*22*). Analytical SAX-HPLC was performed using a 120 min linear gradient of 0 to 1.2 M sodium chloride at pH 3.5. Sample purity was confirmed by the presence of a single symmetrical peak. monitored by absorbance at 232 nm.

(iii) Spectra Analysis of Oligosaccharides. Negative-ion spectra were performed using an electrospray interface. Nitrogen gas was used both as bath and nebulizer gas. Tetraethylammonium iodide in acetonitrile was used as the calibrant. The solutions of dermatan and chondroitin sulfate-derived tetrasaccharides, hexasaccharide and hyaluronan tetrasaccharide were prepared for negative ESI-MS by dissolving the solid sample in 1:1 water/acetonitrile with 0.05% NH_4OH which was also used for the mobile phase. ESI-MS was performed on an Autospec spectrometer from Micromass, Inc. (England), and yielded masses consistent with the structure of each oligosaccharide.

The pure oligosaccharide samples were dissolved in D_2O (99.0%) filtered through a 0.45 μm syringe filter and freeze-dried to remove exchangeable protons. After exchanging the sample three times, the sample was dissolved in D_2O (99.96% of atom). 1D NMR experiments were performed on 700 μL of 0.1−0.5 mM samples at 500 MHz in a 5 mm triple resonance tunable probe at 298 and 313 K. The HOD signal was suppressed by presaturation during 3 s. All 1D and 2D NMR experiments were performed using a Varian 500 MHz NMR spectrometer, and yielded spectra consistent with the structure of each oligosaccharide.

Site-Directed Mutagenesis, Construction of Mutant Strains, and Expression of Proteins. The lyase AC gene [*cslA* (*23*)] with Hep1 upstream regions was cloned in the plasmid pUC21 (*24*). Mutations were introduced using a recombinant PCR strategy. Two primers (5′-TGATGAGGCTTTGCTTTC-3′; 5′-AACTGTGCTATCTGTCCT-3′) were prepared flanking the multiple cloning site of pUC21. The following mutagenic oligonucleotide primer pairs were used to introduce the specified mutations. Bases modified to obtain the desired point mutation are indicated in bold, with those underlined indicating a silent mutation introduced to create a new restriction site to be used as a diagnostic in screening. For His225Ala, 5′-TACGATTATTCCTAC CTGCAG**GC**-CGGCCCGCAATTACAGATATCGAGC-3′; 5′-GCTCGA-TATCTGTAATTGCGGGCCG**GC**CTGCAGGTAGGAA-TAATCGTA-3′; for Arg288Ala, 5′-TATGGATTTTAACG-TAGAAGGC**GC**CGGAGTAAGCCGGCCAGA-3′; 5′-TC-TGGCCGGCTTACTCCG**GC**GCCTTCTACGTTAAAAT-CCATA-3′; for Arg292Ala, 5′-TAGAAGGCCGCGGAG-TAAGT**GCA**CCAGACATTCTAAATAAAAAGGC-3′; 5′-GCCTTTTTATTTAGAATGTCTGG**TGC**ACTTACTC-CGCGGCCTTCTA-3′, and for Tyr234Phe 5′-ACGGTCCG-CAATTACAGATAAGCAGCTTTGGTGCCGTATTTAT-TAC-3′; 5′-CTGGCTATCGCATCAGCCCATTCTTCAG-TAT-3′. Constructs containing the mutated *cslA* genes fused with the *hepA* upstream region were introduced into plasmid pIBXF1 to yield the final constructs for conjugation. These constructs were introduced into *Escherichia coli* strain S17-1 and conjugated into *F. heparinum* to create strains containing the mutant genes (*25*). These constructed strains were confirmed by their ability to grow on medium containing heparin as the sole source of carbon, and by their resistance to the antibiotic trimethoprim. In addition, the mutated codons were further confirmed by sequencing the mutated region amplified by PCR.

Mutant *F. heparinum* strains were grown at 23 °C in minimal medium (*26*) containing 1% (w/v) semi-purified heparin and 100 mg L^{-1} trimethoprim antibiotic. Cells were harvested by centrifugation, resuspended in phosphate buffered saline to approximately 5 OD_{600} mL^{-1} and lysed by sonication (45 s on, 45 s off, five cycles, 4 °C). The soluble protein fraction was isolated by centrifugation (10 000*g*, 4

°C, 10 min) and checked for lyase AC activity with chondroitin-4-sulfate as substrate. Expression of mutant lyase AC proteins was confirmed by SDS−PAGE and Western blotting using polyclonal anti-lyase AC antibodies as previously described (*23*).

Purification of Mutant Proteins. Lyase AC mutants were purified similarly as for the wild-type enzyme (*9*). *F. heparinum* cells from 4 L of culture were resuspended in buffer consisting of 25 mM sodium phosphate, 100 mM NaCl, pH 7, and lysed by high-pressure homogenization at 8000 Pa for three passes. Cell debris was removed by centrifugation (10 000g, 4 °C, 30 min), and 0.5 mM of PMSF or Complete EDTA-free protease inhibitor cocktail tablets, 2 mM $MgCl_2$ and 1 mg/L DNAse I (Sigma) added to the supernatant fraction and incubated 2−4 h at 4 °C.

The protein supernatant was filtered through a 0.45 μm disk filter, diluted 1:4 (vol/vol) with cold 10 mM sodium phosphate buffer, pH 7, and loaded onto a SP−Sepharose Big Beads cation exchange column (1.6 × 35 cm), equilibrated with 10 mM sodium phosphate buffer, pH 7, attached to a Pharmacia FPLC system. After washing with three column volumes of equilibration buffer, bound proteins were batch eluted with 2 column volumes of 25 mM sodium phosphate buffer, 150 mM NaCl, pH 7.0, at a flow rate of 1.5 mL min^{-1}.

Fractions containing lyase AC were pooled, diluted 1:1 (v/v) with 10 mM sodium phosphate buffer, pH 7.0, and applied to a ceramic hydroxyapatite column (1.6 × 11.5 cm) equilibrated with 10 mM sodium phosphate buffer pH 7. The column was washed with 3 column volumes of equilibration buffer, and bound proteins eluted in a linear gradient over 12 column volumes of (10−50% v/v) 25 mM sodium phosphate buffer, 1 M NaCl, pH 7.0, followed by 2 column volumes with 100% (v/v) of the same buffer. Column fractions containing purified protein as judged by SDS−PAGE and that were devoid of heparinase III activity were pooled, desalted by ultrafiltration using centiprep and centricon concentrators, and the buffer exchanged to 20 mM Tris-HCl, pH 8.0. The following protease inhibitors were added at the specified concentration: 0.5 mM PMSF, 1 μg/mL leupeptin, 1 μg/mL aprotinin, and 1 μg/mL E64. Protein samples were stored at −20 °C.

Protein Crystallization and Data Collection. Crystallization of both native and mutant enzymes was performed by the hanging drop vapor diffusion method according to the published protocol (*27*) with minor modifications. The reservoir solution consisted of 15% (w/v) poly(ethylene glycol) (PEG) 3350, 400 mM sodium acetate, 100 mM HEPES buffer, pH 7.5. Hanging drops of 5 μL of protein solution and 5 μL of reservoir solution were suspended over 1 mL of reservoir solution and stored at room temperature (~20 °C). Seeding was preformed within a day of setting the drops. Crystals grew to 0.4 × 0.4 × 0.7 mm^3 in size and belong to space group $P4_32_12$ with cell dimensions $a = b =$ 86.9 Å, $c = 192.3$ Å and $Z = 8$. Poly(ethylene glycol) 3350 at 30% (w/v) was found to be the best cryoprotectant. The oligosaccharide-lyase AC complexes were prepared by soaking crystals for one to 3 days in cryoprotectant solution containing 5 mM DS^{tetra}, DS^{hexa}, CS^{tetra}, or 15 mM HA^{tetra} oligosaccharides. Crystals were scooped in a nylon loop and flash frozen at 100 K in a stream of nitrogen gas using an Oxford Cryosystem (Oxford Instruments, Oxford, U.K.).

Table 1: Data Collection Statistics

	dataset[a]			
	DS^{hexa}	DS^{tetra}	HA^{tetra}	CS^{tetra}
sugar concentration (mM)	5	5	15	5
soaking time (days)	3	3	3	1
resolution (Å)	20−2.0	20−2.0	20−2.1	20−2.3
total reflections	204 934	282 695	265 815	178 404
unique reflections	48 610	49 755	43 620	33 117
completeness (%, last shell)	96.2 (87.6)	98.6 (98.1)	99.3 (98.0)	99.6 (99.8)
R_{sym}[b] (%, last shell)	6.5 (24.4)	6.3 (30.2)	8.2 (26.9)	6.4 (26.7)
mean $I/\sigma I$	15.8	14.3	14.0	15.4

[a] Datasets DS^{hexa}, DS^{tetra}, and HA^{tetra} are for native lyase AC crystals. Dataset CS^{tetra} is with the Tyr234Phe mutant of lyase AC. [b] $R_{sym} = \sum h \sum i \mid I(h,i) - \langle I(h) \rangle \mid / \sum h \sum i I(h,i)$, where $I(h,i)$ is the intensity of the ith measurement of h, and $\langle I(h) \rangle$ is the corresponding mean value of h over all i measurements of h, with the summation being over all measurements.

Diffraction data were collected using a Quantum-4 CCD detector at the X8C beamline, NSLS, Brookhaven National Laboratory. The crystals were oriented with their *c* axis approximately parallel to the spindle and 1.0° oscillation frames collected. Data were processed with the programs DENZO and SCALEPACK (*28*). Data collection statistics are presented in Table 1.

Crystallographic Refinement and Model Validation. The structures of lyase AC−DS^{tetra}, DS^{hexa}, HA^{tetra}, and CS^{tetra} complexes have been refined at 2.0, 2.0, 2.1, and 2.3 Å resolution, respectively. The crystals of these complexes are isomorphous to the native crystals (*18*) and therefore the native lyase AC molecule was used as the starting model. Since the freezing conditions differed from those used in the original structure determination, we re-refined the native structure against a new native data set collected under the same conditions as the complexes. This structure was used for all comparisons described in this paper. In all cases, model building was performed with the program O (*29*). The complexes have been refined using the program CNS (*30*) using a maximum likelihood target against all data and a bulk solvent correction. In each dataset, 3% of the reflections were set aside to monitor R_{free} during the progress of refinement. The refinement protocol included positional refinement, simulated annealing and finally individual *B*-factor refinement. The oligosaccharides present at the two glycosylation sites, Ser328 and Ser455, were added and placed in well-defined electron density. At the Ser328 site three sugars were included, while for the Ser455 site five sugars were modeled. Subsequent $F_o - F_c$ and $2F_o - F_c$ electron density maps clearly showed the location of the bound oligosaccharides. Three N-terminal residues and one C-terminal residue were disordered in all of the complexes and were not included in the final models. Final refinement statistics are presented in Table 2. The final models were analyzed with PROCHECK (*31*) and have been deposited in the Protein Data Bank.

RESULTS AND DISCUSSION

Overall Structure of the Complexes. Enzyme−oligosaccharide complexes have been obtained by soaking lyase AC crystals in a cryoprotectant solution containing milimolar concentrations of specific oligosaccharides (Table 1). This

Table 2: Statistics of Crystallographic Refinement

soaked sugar	dataset			
	DS^{hexa}	DS^{tetra}	HA^{tetra}	CS^{tetra}
observed in map	DS^{tetra}	DS^{di}	HA^{di}	CS^{tetra}
resolution (Å)	20−2.0	20−2.0	20−2.1	20−2.3
no. of reflections (working set)	45 504	47 023	41 110	30 593
no. of reflections (test set)	1627	1452	1280	934
R_{work}[a]	0.233	0.227	0.226	0.219
R_{free}[b]	0.270	0.266	0.254	0.275
no. of protein atoms	5383	5383	5383	5383
no. of covalent sugar atoms [avg *B*-factor (Å^2)][c]	85 (42.7)	85 (35.8)	85 (39.1)	85 (60.8)
no. of noncovalent sugar atoms [avg B-factor (Å^2)][d]	61 (46.7)	30 (28.4)	27 (30.1)	60 (61.0)
no. of waters [avg *B*-factor (Å^2)]	313 (31.4)	381 (28.3)	327 (30.4)	326 (43.5)
avg *B*-factor [protein (Å^2)]	28.1	22.3	25.7	42.0
Ramachandran plot				
most-favored regions (%)	85.3	87.2	86.2	84.0
generously allowed regions (%)	0.7	0.8	0.8	0.3
disallowed regions	0.0	0.0	0.0	0.3

[a] $R_{work} = \sum | F_{obs} - F_{calc}| / \sum F_{obs}$. [b] $R_{free} = R_{work}$, but for a random test set of 3% of reflections not included in the refinement. [c] Number of sugar atoms and *B*-factors for protein glycosylation sites (Ser328 and Ser455). [d] Number of sugar atoms and *B*-factors for sugars bound at the active site.

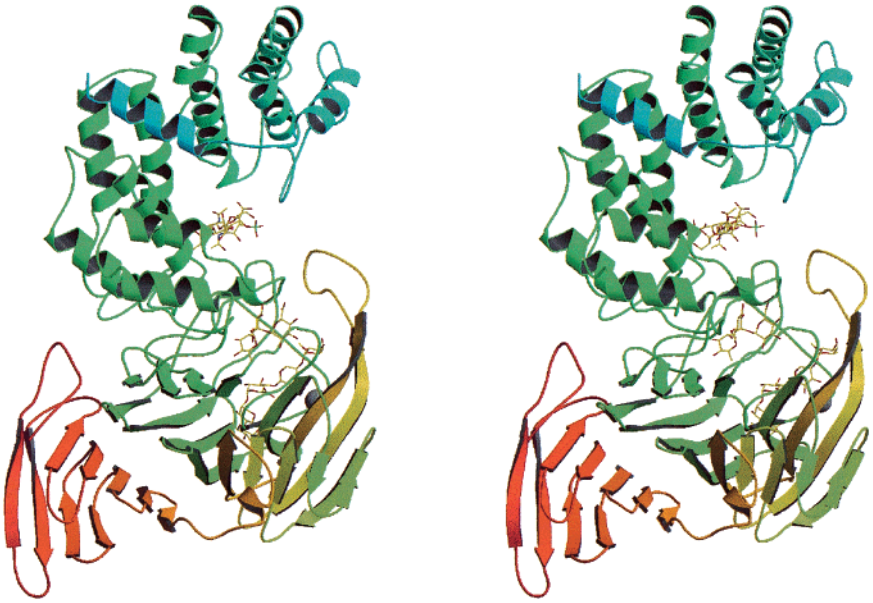

FIGURE 2: Ribbon drawing of lyase AC showing the position of bound DS^{hexa}. The N- and C-terminal domains are shown in different colors. The dermatan tetrasaccharide modeled from DS^{hexa} is shown in ball-and-stick representation.

cryoprotectant solution was somewhat different from that used in the original structure determination (*18*). The root-mean-squares (rms) deviation between the Cα coordinates of the present and published native models is 0.29 Å, indicating that no significant structural changes have occurred. Similarly, the rms deviation between the native lyase AC and the complexes is small and varies between 0.07 and 0.30 Å for all Cα atoms. Therefore, soaking in the oligosaccharides had little effect on the overall structure of the enzyme. Analysis of the diffraction data for the various complexes using a Wilson plot gave overall temperature factors of 18.7, 17.2, 17.8, and 37.8 Å^2 for the DS^{hexa}, DS^{tetra}, HA^{tetra}, and CS^{tetra} complexes, respectively. This indicates that the higher individual B-factors from refinement for the CS^{tetra} complex are inherent within the diffraction data itself.

Four oligosaccharides were used in this study: a dermatan sulfate hexasaccharide (DS^{hexa}), dermatan sulfate tetrasaccharide (DS^{tetra}), hyaluronic acid tetrasaccharide (HA^{tetra}), each bound to native AC lyase, and a chondroitin 4,6-sulfate tetrasaccharide (CS^{tetra}) bound to the lyase AC mutant Tyr234Phe (Figure 1). Hyaluronic acid lacks the sulfation typical for chondroitin and dermatan sulfates and its hexose is a GlcNAc rather than a GalNAc (different configuration at the C4 position). Despite these differences, hyaluronic acid is degraded by lyase AC. Similar cross-specificity is observed for hyaluronate lyases, which retain activity on chondroitin (*8*).

Lyase AC is composed of two domains (Figure 2). The N-terminal domain (residues 24−335) consists of five helical hairpins forming a incomplete double-layered $(\alpha/\alpha)_5$ toroid, as classified within the SCOP database (*32*), with a long, deep groove on one side. This structural arrangement, including the presence of a large cleft, is very similar to that observed for two other polysaccharide lyases, that of alginate lyase A1-III from *Sphingomonas* species A1 (*19*) and the N-terminal domain of *S. pneumoniae* hyaluronate lyase (*14*).

In the lyase AC structure, the helices are inclined relative to the axis of the toroid, coming closer together at one end. An additional α-helix at the N-terminus lies across the wider opening of the toroid and constricts one end of the groove. The C-terminal domain (residues 336−700) is composed of four extensive β-sheets (*18*). The surface interacting with the N-terminal domain is composed mostly of the residues from the largest β-sheet and its protruding loops and contacts the narrow end of the toroid. These loops enclose the end of the groove in the N-terminal domain but do not block it off completely. A narrow tunnel leads from the narrow end of the groove to the exterior of the protein.

In all four complexes, electron density corresponding to the oligosaccharides was found in the same region of the molecule. As was expected from the surface topology and pattern of sequence conservation, they are bound in the groove within the N-terminal domain near its narrow end and in the vicinity of the conserved residues His225, Tyr234, Arg288, and Arg292. These amino acids were previously predicted to contribute to the active site (*18*). Part of this substrate-binding site is lined with residues from the C-terminal domain. With the exception of the CS^{tetra} complex, not all of the sugars are visible in the final electron density maps. Only four sugar units were sufficiently well defined to be modeled for DS^{hexa}, two for DS^{tetra} and two for HA^{tetra} (Figure 3). With the CS^{tetra} complex bound to the Tyr234Phe mutant of lyase AC, all four sugar rings showed clear electron density. The well ordered sugar units from different complexes were not only bound in the same region of lyase AC, but the disaccharide units superpose well (Figure 3c). Indeed, the disaccharide unit of DS^{tetra} superposes with the disaccharide unit at the nonreducing-end of DS^{hexa}, maintains the same conformation and makes many of the same contacts with the enzyme (Table 3). For these reasons, we only discuss the DS^{hexa} complex in detail. The disaccharide unit of HA^{tetra} also superposes with the disaccharide unit located at the nonreducing end of DS^{hexa}; however, the GlcUA moiety of HA^{tetra} assumes a different conformation ($^4C_1$) than the IdoUA ($^1C_4$) of DS^{hexa}, resulting in somewhat different protein oligosaccharide interactions. These differences in uronic acid conformation are also visible comparing the DS^{hexa} and CS^{tetra} structures (Table 3, Figure 3).

Enzyme−Oligosaccharide Interactions. (i) Structure of the Lyase AC-DS^{hexa} Complex. The four ordered sugars of DS^{hexa} adopt a fully extended conformation with the long axis of the chain nearly parallel to the axis of the $(\alpha/\alpha)_5$ torus. The mean planes of the sugars within the disaccharide repeating unit are oriented roughly the same way; however, the two disaccharide units are related approximately by a 2-fold screw axis, consistent with the 2_1 helical crystal structure of dermatan sulfate determined by fiber diffraction (*33*). As expected for dermatan sulfate, the GalNAc units have the $^4C_1$ conformation, and the IdoUA are $^1C_4$, respectively (*34*). Of the four ordered sugar units, the two sulfated GalNAc residues are the best defined in the electron density map (Figure 3a). The position of the remaining disaccharide could not be discerned from the experimental electron density maps. The oligosaccharide is bound near the narrow end of the groove, which is enclosed by the loops from the C-terminal domain. The DS^{hexa} oligosaccharide is found occupying the tunnel, with its reducing end protruding to the exterior of the protein surface (Figure 4).

Table 3: Direct Polar Contacts (≤3.7 Å) between Lyase AC and DS^{hexa}, DS^{tetra}, or HA^{tetra} Oligosaccharides and Lyase AC Tyr234Phe Bound to CS^{tetra} [a]

sugar		protein	distance (Å)			
residue	atom	side chain	DS^{hexa}	DS^{tetra}	HA^{tetra}	$CS^{tetra(4S,6S)}$
$IdoUA^{708}$ or	O2	$Arg292^{NH1}$			3.44	3.34
$GlcUA^{708}$	O3	$Arg292^{NH1}$	3.52			
$GalNAc^{709}$	O1	$Arg288^{NH2}$		2.94	3.09	
	O1	$Tyr234^{OH}$		3.07	3.24	
	O3	$Arg292^{NH1}$			3.23	3.45
	O5	$Arg288^{NH2}$	3.54		3.68	
	O7	$Arg292^{NH1}$	3.02*	3.10*	3.10*	3.11*
	O7	$Arg292^{NH2}$	2.90*	2.96*	3.67	2.64*
	O7	$Arg288^{NH2}$	3.64	3.70		3.43
	SO43	$Arg292^{NH1}$	3.58	3.66		
	SO43	$Arg292^{NE}$	3.09*	3.14		3.51
	SO43	$Arg292^{NH2}$	3.54	3.58		
$IdoUA^{710}$ or	O2	$Asn374^{OD1}$	3.09			
$GlcUA^{710}$	O2	$Asn374^{ND2}$	2.80*			3.30*
	O2	$Asn125^{ND2}$				3.49
	O2	$Arg288^{NH2}$	2.36*			
	O3	$Asn125^{ND2}$	3.36			2.84*
	O3	$Asn125^{OD1}$	3.06*			3.68
	O4	$Arg288^{NH2}$	3.22			2.69*
	O4	$Tyr234^{OH}$	3.43			
	O5	$Tyr234^{OH}$	2.81*			
	O5	$His225^{NE2}$	3.28			
	O6A	$Asn175^{OD1}$	2.62*			
	O6A	$Tyr234^{OH}$	3.35			
	O6A	$Asn175^{ND2}$	2.66*			
	O6A	$His225^{NE2}$	3.53			3.42
	O6A	$Arg288^{NH1}$				2.66*
	O6A	$Arg288^{NH2}$				3.52
	O6B	$Asn175^{OD1}$	2.96*			
	O6B	$Trp127^{NE1}$	3.43			
	O6B	$His225^{NE2}$				3.64
$GalNAc^{711(4S)}$ or	O3	$Trp126^{NE1}$				3.31
$GalNAc^{711(6S)}$	O7	$Trp126^{NE1}$	3.60			3.49
	SO41	$Asn175^{ND2}$	3.68			
	SO42	$Asn175^{ND2}$	2.99*			
	SO42	$His225^{NE2}$	2.80*			
	SO62	$Trp427^{O}$				3.52
	SO43	$Asn175^{ND2}$	3.25			

[a] Residues involved in hydrogen bonds are indicated by an asterisk (*).

In our description of the substrate and substrate-binding site we adopt the nomenclature of Davies, Wilson and Henrissat (*35*). Accordingly, the sugars are numbered starting from the cleavage point, with the positive numbers increasing toward the reducing end of the oligosaccharide, and the negative numbers decreasing toward the nonreducing end (nonreducing end, ..., −3, −2, −1, +1, +2, +3, ..., reducing end). Based on the present structure, residue conservation pattern and the proposed reaction mechanism, the ordered tetrasaccharide occupies subsites −2, −1, +1, and +2. Sulfated GalNAc binds to subsites −1 and +2, while IdoUA bind to subsites −2 and +1. This extended substrate binding site is formed by residues from both domains (Figure 5a). The most extensive protein-carbohydrate interactions are formed by the two GalNAc residues located at the −1 and +2 subsites, and by the +1 IdoUA. The enzyme interacts with oligosaccharides only through protein side chains; there are no main chain interactions. Several water molecules contribute to binding through bridging interactions between sugar moieties and the protein. The IdoUA at subsite −2 lies in the wider part of the groove and forms few direct contacts with the enzyme. Rather, it interacts with the enzyme

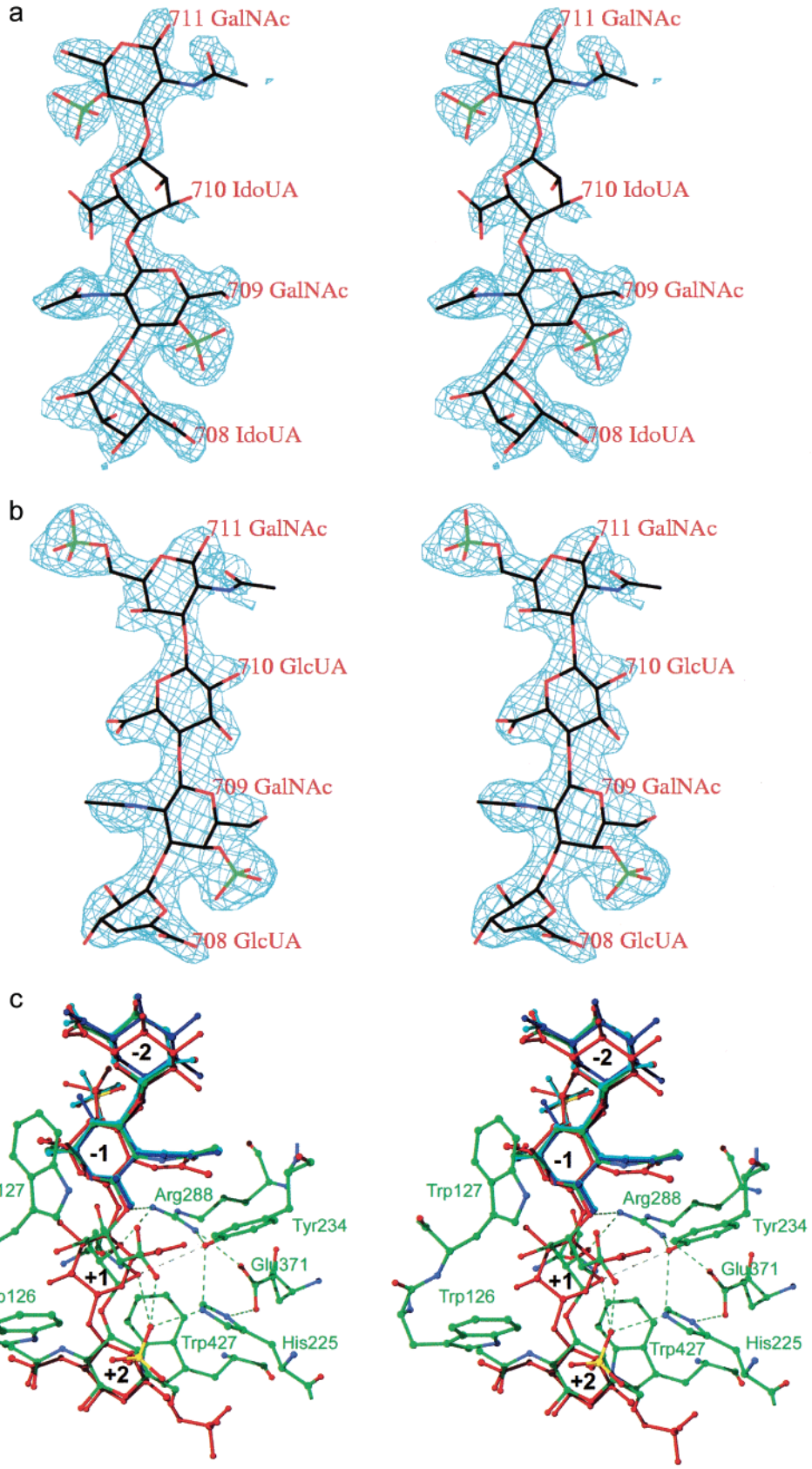

FIGURE 3: Stereoview of the $2mF_o - DF_c$ electron density based on the final refined coordinates for (a) lyase AC bound to DS^{hexa}, (b) lyase AC Tyr234Phe bound to CS^{tetra}, and (c) overlap of GAGs from the DS^{hexa}, DS^{tetra}, HA^{tetra}, and CS^{tetra} complexes based on the superposition of 20 residues contacting or in the proximity of the bound oligosaccharide. The reducing end of the oligosaccharide is at the bottom, the cleavage occurs between −1 and +1 sugars. The key residues of lyase AC involved in binding and catalysis are included in the figure. DS^{hexa} is colored by atom colors, CS^{tetra} is red, DS^{tetra} is cyan, HA^{tetra} is blue. Hydrogen bonds are shown as green dashed lines. The catalytic tetrad, His225, Tyr234, Arg288, and Glu371, is connected by a network of hydrogen bonds. This figure was generated with program sPDBViewer (*54*) and POV−Ray (http://www.povray.org/).

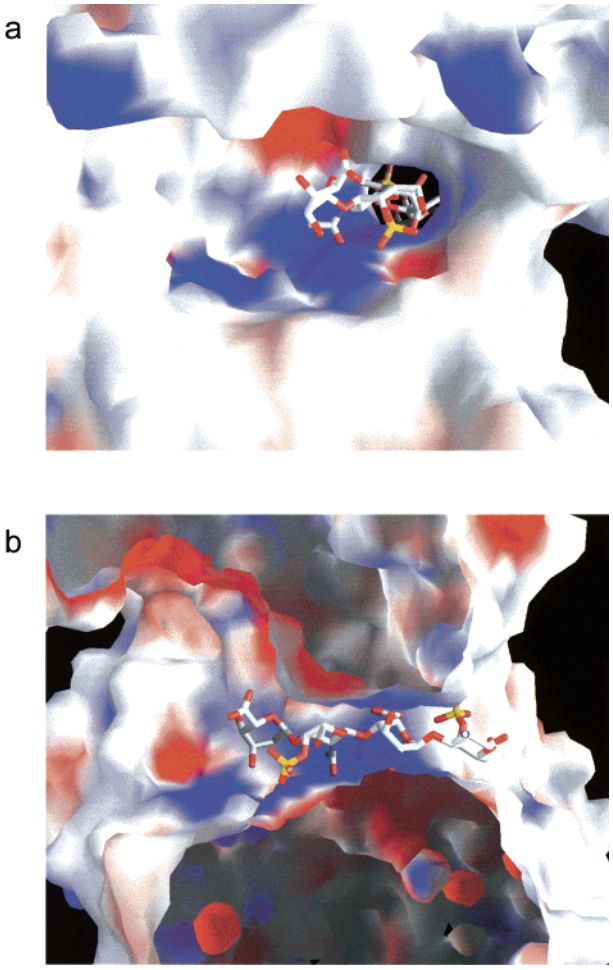

FIGURE 4: (a) Surface representation of lyase AC Tyr234Phe bound to CS^{tetra}, showing the electrostatic potential and the oligosaccharide protruding through the tunnel at the molecular surface. The bottom of the tunnel has a positive potential. (b) Cut-away view of the CS^{tetra} oligosaccharide bound within the tunnel in which the residues forming the loops Asp71-Trp76 and Gly373-Lys375 have been largely removed. This view is related by an ~90° rotation along the vertical axis to the view above. Figures were prepared using the program GRASP (*55*).

through bridging water molecules. It thus appears that the enzyme utilizes only three subsites to recognize the substrate: −1, +1, and +2, and that side chains from both domains are required to form a fully functional active site.

The electrostatic surface of the groove within the substrate binding area shows that the sulfate binding sites indeed have positive potential and that there is charge complementarity between the disaccharide repeating unit and the groove. Interactions between GAG molecules and proteins are often dominated by both polar and positively charged residues, particularly arginine (*36*). Another prominent feature of the substrate-binding site is the presence of three tryptophan residues. Trp127 (N-terminal domain) stacks against the hydrophobic face of the −1 GalNAc and Trp427 (C-terminal domain) stacks against the apolar side of the +2 GalNAc from the opposite face of the oligosaccharide chain (Figure 3c). This type of interaction is often found in the carbohydrate binding sites of proteins (*37*, *38*) and are observed in the interaction between hyaluronate lyase and hyaluronan disaccharide (*15*). The ring of the third tryptophan, Trp126, is perpendicular to the oligosaccharide chain and together with Trp427 holds the +2 GalNAc tightly in place. Many

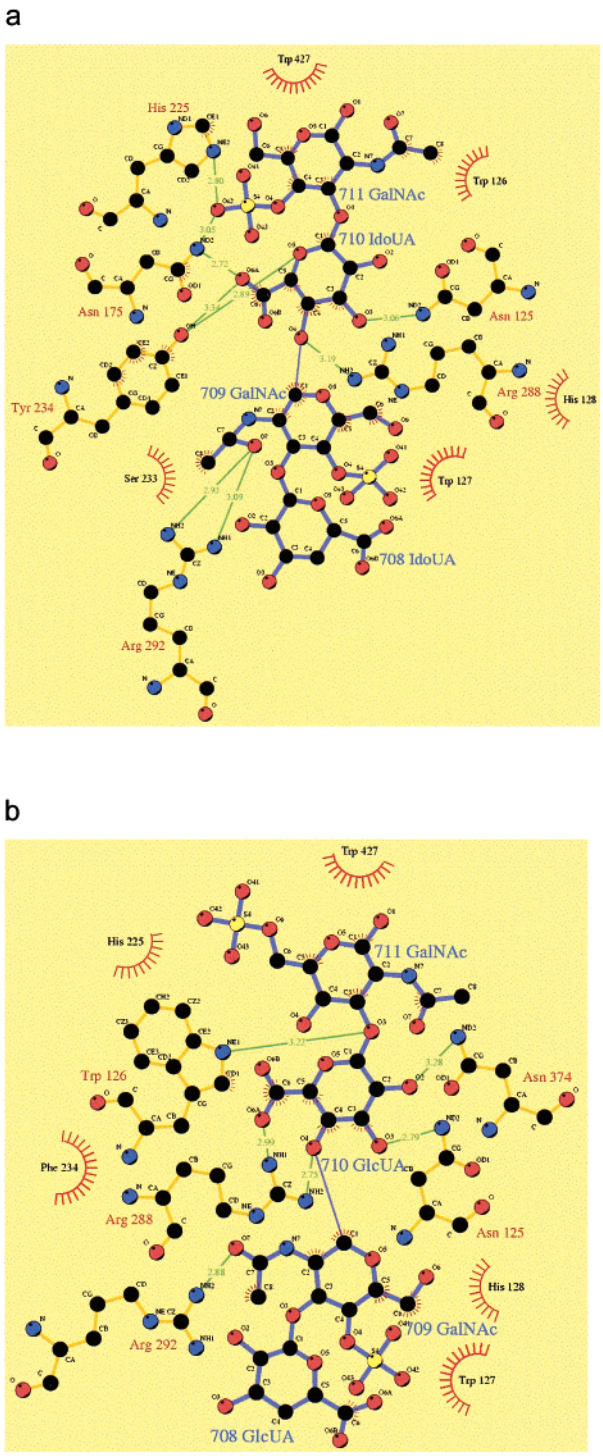

FIGURE 5: Schematic representation showing residues contacting bound oligosaccharide in (a) lyase AC−DS^{hexa} complex, and (b) lyase AC Tyr234Phe mutant-CS^{tetra} complex. Only hydrogen bonds between the oligosaccharide and the protein are shown (green lines). Three residues of the catalytic tetrad are shown: His225, Tyr234, and Arg288. The fourth, Glu371 is not shown here, as it does not contact directly the oligosaccharide. The figure was prepared with the program Ligplot (*56*).

of the residues within the binding cleft that make interactions with oligosaccharides are also conserved in bacterial hyaluronate lyases [Figure 6 (*15*, *16*, *18*)].

The −1 subsite is formed by the side chains of Thr74, Asn125, Trp127, His128, Ser233, Tyr234, Arg288, Arg292, and Glu376. GalNAc in this subsite maintains several hydrogen bonds to the enzyme, either directly or through

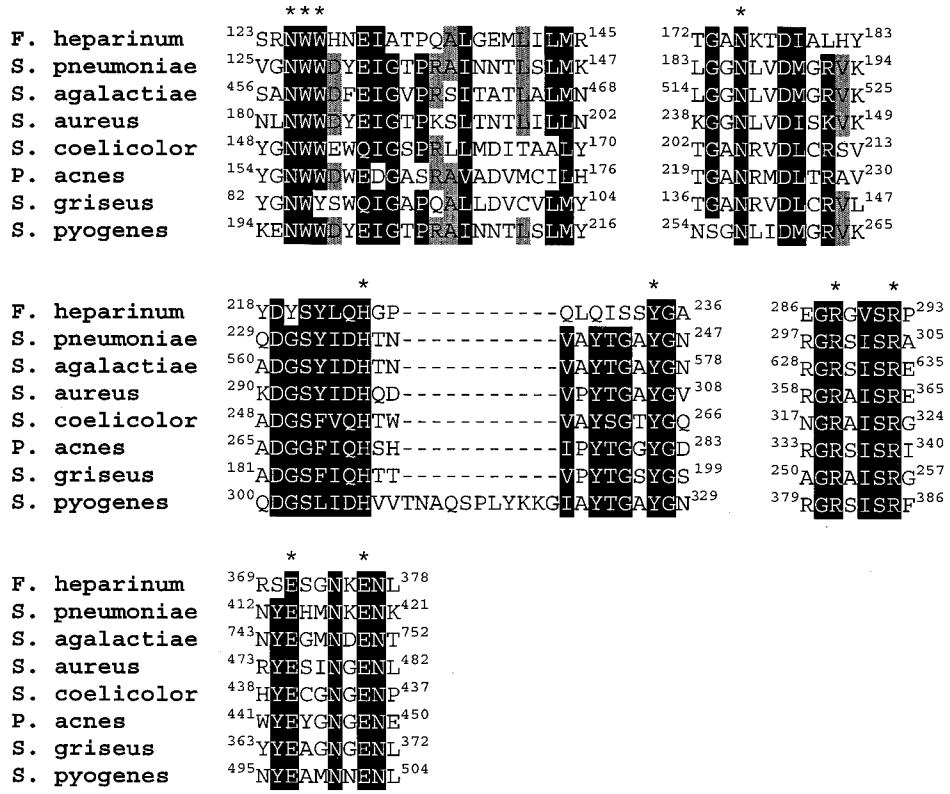

FIGURE 6: Selectedsequence alignment of lyase AC and bacterial hyaluronate lyases showing conservation of key active site residues. Identical or highly conserved residues are shaded in black, with residues making contacts with DS^{hexa} indicated by an asterisk (*). Numbering of the protein sequence corresponds to the full-length form of each enzyme. The sequences and corresponding NCBI accession numbers (in brackets) are for *F. heparinum* AC lyase (GI:1002524); *Streptococcus pneumoniae* hyaluronidase (GI:437704); *Streptococcus agalactiae* hyaluronate lyase (GI:3287245); *Staphylococcus aureus* hyaluronate lyase (GI:705405); *Streptomyces coelicolor* hyaluronate lyase (GI:7479266); *Propionibacterium acnes* hyaluronidase (GI:562085); *Streptomyces griseus* hyaluronate lyase (GI:5002504); and *Streptococcus pyogenes* hyaluronate lyase (GI:6851375). Alignment was performed with the program CLUSTALW (*57*).

bridging water molecules. The 4-sulfate group of GalNAc is bridged by two water molecules to Ser552 and His553 (C-terminal domain) and is located directly above the guanidinium group of Arg292. This arginine is kept in the proper orientation by a salt bridge to Glu376. In addition to the electrostatic interactions with the sulfate group, Arg292 interacts directly with the −1 GalNAc pyranose ring and makes two hydrogen bonds to the acetyl group. The nitrogen atom of this group is hydrogen bonded to a water molecule. The 6-hydroxyl group forms a hydrogen bond to a water molecule, WAT933, which in turn is hydrogen bonded to the side chains of Arg288 of the N-terminal domain, and Asn374 and Glu376 of the C-terminal domain, forming a tetrahedral arrangement. This solvent molecule is present also in the native structure. The O1 oxygen atom in the glycosidic linkage between the −1 and +1 sugars is also within hydrogen bonding distance to the $NH2^{Arg288}$ atom.

The +1 subsite is located in the narrower part of the tunnel and is bound by the side chains of Asn125 Trp126, Asn175, His225, Tyr234, Arg288, and Asn374. The ring is in a $^4C_1$ chair conformation with an equatorial C5 carboxylate group and the remaining substituents in axial orientations. All of the oxygen atoms of IdoUA are involved in hydrogen bonds: 2-OH to the side chains of Arg288 and Asn374, 3-OH to Asn125, O5 to the hydroxyl of Tyr234, and the carboxylic group to Asn175 and to a water molecule (Figure 5a; Table 3). Two key residues, Arg288 and His225, are precisely positioned through formation of hydrogen bonds with Glu371 of the C-terminal domain, a residue conserved between lyase AC and bacterial hyaluronate lyases (Figure 6).

The GalNAc at the +2 subsite is bound through interactions with Trp427 and Trp126 and by hydrogen bonds of the 4-sulfate group to His225, Asn175, and the carboxylate of the +1 iduronic acid. Another side chain in the proximity is that of Lys171.

(ii) Structure of the Lyase AC−DS^{tetra} Complex. As noted previously, the DS^{tetra} is partially disordered with the two visible sugars occupying the −2 and −1 subsites. Many of the interactions with the enzyme are the same as those made by DS^{hexa} (Table 3). Comparison with DS^{hexa} clearly suggests that the disordered disaccharide of DS^{tetra} is located at the nonreducing end within the wide part of the groove. Had this disaccharide occupied subsites +1 and +2, it would have been ordered due to the steric restrictions imposed by these sites. Both the DS^{tetra} and DS^{hexa} oligosaccharides contain an unsaturated nonreducing end, so in principle it is possible to structurally distinguish the two disaccharide-repeating units. Higher resolution data, however, are required to clearly make this distinction.

(iii) Structure of Lyase AC−HA^{tetra} Complex. Unlike DS^{tetra} and DS^{hexa}, the HA^{tetra} oligosaccharide was prepared such that it is saturated at its nonreducing end. Although HA^{tetra} was soaked into the crystal, the electron density was clear for only a disaccharide. This is similar to the results obtained with DS^{tetra}. However, since lyase AC exhibits activity toward hyaluronan, a second possibility is that the HA^{tetra} has been enzymatically cleaved in the crystal. The result of this would

be the presence of one disaccharide unit, which we observe in the crystal structure.

The disaccharide binds within the groove in the same location as DS^{tetra}, corresponding to the −2 and −1 subsites. The GlcNAc occupies the −1 subsite, and although it lacks the 4-sulfation, its sugar ring superimposes almost perfectly on that of GalNAc found in dermatan sulfate (Figure 3c). We observe the same stacking interactions with Trp127 as with DS^{tetra} and DS^{hexa}. Similarly, the 6-OH of GlcNAc makes a hydrogen bond to a bridging water molecule, WAT933, fixed by interactions with Arg288, Asn374, and Glu376. The *N*-acetyl group is hydrogen bonded to Arg292 and to a water molecule. The configuration at the C4 atom is opposite to that found in dermatan sulfate, with an equatorial hydroxyl group instead of an axial sulfate group. This hydroxyl forms a hydrogen bond to O5 of the neighboring GlcUA and to a water molecule. Comparing the binding of GlcNAc and 4-sulfated GalNAc at the −1 subsite one may conclude that the determining factor is the stacking with Trp127 rather than interactions with the sulfate group.

The sugar at the −2 subsite is GlcUA rather than IdoUA as found in the DS^{tetra} and DS^{hexa}. While IdoUA has the $^1C_4$ conformation, with all substituents except the carboxylic group axial to the ring, GlcUA adopts the $^4C_1$ conformation, with all substituents equatorial. As with the lyase AC−DS^{hexa} and −DS^{tetra} complexes, this sugar makes very few direct contacts with the enzyme and instead hydrogen bonds with ordered water molecules.

Structure of the Lyase AC Tyr234Phe Mutant Bound to $CS^{tetra.}$ To experimentally determine the mode of binding of the natural substrate to lyase AC, crystals of the Tyr234Phe mutant were prepared, and soaked in cryoprotectant solution containing chondroitin sulfate tetrasaccharide. Interpretable electron density was obtained for all four sugar rings (Figure 3b) and allowed a model to be built of the mutant enzyme−oligosaccharide complex (Figures 3c and 5b). The two disaccharide units are related by a 2_1 screw axis, as observed with dermatan sulfate, with both the GalNAc and GlcUA sugars in the $^4C_1$ conformation (*34*). The CS^{tetra} binds at an identical location within the active site tunnel as observed for the tetrasaccharide of DS^{hexa}. This result suggests that Tyr234 has a primary role in catalysis, as the Tyr234Phe mutant retains its ability to bind substrate. Comparing the bound DS^{hexa} and CS^{tetra} oligosaccharides, the positions of the bound GalNAc sugars are very similar, although, as expected, the conformations of the IdoUA and GlcUA rings differ.

Superposition of lyase AC Tyr234Phe bound to CS^{tetra} with the native lyase AC shows that the carboxylic group of GlcUA bound at the +1 subsite occupies the space of the hydroxyl group of Tyr234 of the native enzyme. We have modeled native lyase AC bound to CS^{tetra} by rotating the glycosidic bonds on either side of the +1 GlcUA in order to avoid steric conflicts with Tyr234 (Figure 3c). Molecular mechanics calculations on the isolated CS^{tetra} indicate that this rotation increases the conformational energy and suggests that binding of the substrate to the native enzyme is associated with a certain conformational strain. It is likely that this sterically strained conformation represents the catalytically competent state of the oligosaccharide, and that this torsional strain in some way contributes to catalysis.

While several of the lyase AC−oligosaccharide polar contacts are conserved between dermatan and chondroitin sulfate, there are nine new contacts observed between CS^{tetra} not observed for DS^{hexa}, most of which involve the disaccharide at the reducing end (Table 3). At the same time, 12 polar contacts formed between lyase AC and DS^{hexa} are not observed in the lyase AC−CS^{tetra} complex. While the 4-sulfo group of GalNAc located at the +2 subsite of DS^{hexa} makes hydrogen bonds to $ND2^{Asn175}$ and $NE2^{His225}$, respectively, the 6-sulfo group of CS^{tetra} makes only a weak interaction with the carbonyl O of Trp427. This weaker interaction may account, in part, for the lower activity of lyase AC on chondroitin-6-S as compared to chondroitin-4-S.

Implications for the Mode of Action of Lyase AC. Studies on the mode of action of *F. heparinum* lyase AC show that this enzyme cleaves the chondroitin chain in a random, endolytic manner, yielding a mixture of disaccharides, tetrasaccharides and longer oligosaccharides as the terminal products (*7*, *9*; I. Capila and R.J.L., unpublished results). This mode of action is surprising, given the observed tunnel-like binding sites for oligosaccharides as seen from the cocrystal structures presented here. Most, but not all polysaccharide degrading enzymes having tunnel-like active sites, such as the cellobiohydrolases, possess an exolytic mode of action (*39*). At least one enzyme, the Cel48F cellulase from *Clostridium celluloyticum*, possesses a 25 Å tunnel within its catalytic domain (*40*), but shows a processive, endolytic action pattern. *Streptococcus pneumoniae* hyaluronate lyase yields only disaccharide as the terminal product (*14*) and therefore may have an exolytic mode of action, although it is not clear whether this enzyme possesses a similar active site tunnel as seen in lyase AC.

Comparison of the DS^{hexa} and DS^{tetra} complexes implies that the oligosaccharides bind initially within the groove and migrate to the −2 and −1 subsites. We suggest that these subsites represent a high-affinity substrate recognition area, and the +1 and +2 subsites a product release area (*41*). It is worth considering why DS^{tetra} does not occupy the +1 and +2 subsites. A possible explanation is that a short oligosaccharide can become trapped in the high affinity −1 subsite and cannot overcome the energy barrier necessary to move to the "+" subsites. A longer oligosaccharide has a free tail whose random movements may provide the necessary entropic contribution to jump to the next set of subsites. This mechanism may be valid for free oligosaccharides but would not apply to the GAG chain of a proteolglycan, which is attached at the reducing end to the core protein. Therefore, another explanation has to be considered, namely, that the tunnel is not rigid but that the loops are flexible and open periodically, thereby allowing the glycosaminoglycan chain to slide in, followed by closing of the loops. Inspection of the structure indicates that such an opening would only involve the tips of one or two loops, namely Asp71-Trp76 of the N-terminal domain, and Gly373-Lys375 of the C-terminal domain. In the tunnel-like active sites of cellobiohydrolases, structural evidence for local conformational changes upon polysaccharide binding (*42*, *43*) have been documented. Opening of the tunnel is a likely requirement for the initial endolytic attack of CelF on cellulose (*44*).

Mutagenesis of Putative Catalytic Residues. Within the lyase AC active site region five side chains, Asn175, His225, Tyr234, Arg288, and Arg292, are in close proximity to the

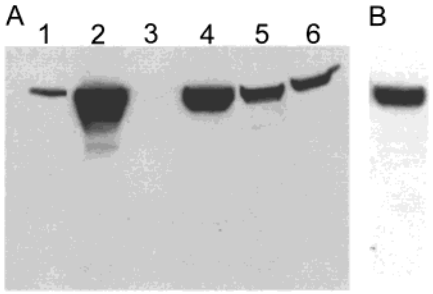

FIGURE 7: Western blot depicting expression of chondroitin AC lyase mutants. (a) Lane 1, 2 μg of purified *F. heparinum* chondroitin AC lyase; lane 2, *F. heparinum* transconjugate lyase AC; lane 3, *F. heparinum* wild-type; lane 4; Arg288Ala; lane 5; Arg292Ala; lane6, His225Ala (b) Tyr234Phe. Approximately 30 μL of cell sonicate supernatant ($OD_{600} = 0.15$) was loaded per lane and probed with polyclonal anti-chondroitin AC lyase antibody. Protein expression was performed as described under Materials and Methods.

scissile bond. Four of these amino acids were targeted for site-directed mutagenesis. Strains of *F. heparinum* overexpressing the His225Ala, Tyr234Phe, Arg288Ala, and Arg292Ala lyase AC mutants were constructed, allowing purification of the mutant proteins and determination of enzymatic activity. These proteins were purified to apparent homogeneity as determined by SDS−PAGE using a combination of SP−Sepharose and hydroxyapatite chromatography, essentially as for the native enzyme. They showed similar elution patterns from hydroxyapatite, eluting in the gradient between 0.14 and 0.22 M NaCl. In each case a small amount of heparinase III was found to elute slightly after the main lyase AC peak from SP−Sepharose, and slightly before the main peak in hydroxyapatite chromatography. Lyase AC and heparinase III have similar molecular masses of 74.5 and 73.5 kDa, respectively, appear as a closely spaced doublet on SDS−PAGE gels and can be readily distinguished in Western blots using anti-lyase AC polyclonal antibodies (results not shown). Determining the heparinase III activity in fractions eluting from the hydroxyapatite column permitted pooling of mutant chondroitin lyase AC proteins free of this activity. The purity of the Arg288Ala and Tyr234Phe mutants was verified by the ability of these proteins to readily yield large single crystals with cell dimensions very close to those of the native enzyme.

Analysis of the His225Ala mutant by SDS−PAGE and Western blotting using polyclonal anti-lyase AC antibodies showed that this protein degraded while at 4 °C within a short time after purification. This presumably resulted from a residual protease activity that co-purified with the enzyme and was able to function despite the presence of a cocktail of protease inhibitors. This mutant was found to be unusually sensitive to proteolytic degradation, although all of the enzymes showed some degradation when stored at −20 °C for several months.

The level of expression of lyase AC mutants was evaluated in supernatants after sonication by Western blot analysis using an antibody specific for lyase AC (Figure 7). All mutants were expressed at a level similar to that of the transconjugate lyase AC. Lyase AC from wild-type *F. heparinum* could not be detected in the Western blot for cells grown in heparin-only medium (Figure 7, lane 3), indicating that the level of lyase AC expression in wild-type *F. heparinum* is very low. Activity assays in these crude extracts showed very low chondroitin-4-sulfate degrading activity for mutants His225Ala, Arg288Ala, and Tyr234Phe. The specific activity of the His225Ala mutant in crude extracts was measured to be 0.058 IU mg^{-1}, less than 1% of the native enzyme activity. Activity measurements for the purified mutants confirmed these results and provided an upper limit for the specific activity of the His225Ala, Tyr234Phe, and Arg288Ala mutants to be at least 2 orders of magnitude less than the native enzyme (Table 4).

Table 4: Enzymatic Activities[a] of Chondroitin AC Lyase Mutants

enzyme	Chon-4-S[b]	Chon-6-S[b]	HA[b]	HS[b]	DS[b]
transconjugate	123.9	62.5	94.5	0.18	0.20
Arg292Ala	21.2	9.54	3.63	0.077	0.012
Arg288Ala	0.94	0.55	0.45	0.038	0.00
Tyr234Phe	0.53	0.23	0.30	0.12	0.028
His225Ala	0.031	0.00	ND	ND	ND

[a] Specific activity is given as IU mg^{-1} protein. [b] Substrate concentrations in each case are 0.5 mg mL^{-1} prepared in 50 mM Tris-Cl buffer, pH 8.0. The substrates are Chon-4-S, chondroitin-4-sulfate; Chon-6-S, chondroitin-6-sulfate; HA, hyaluronic acid; HS, heparan sulfate; DS, dermatan sulfate. ND, not determined.

Implications for the Catalytic Mechanism. Previous proposals for the reaction mechanism catalyzed by various polysaccharide lyases (*5*, *10*−*16*, *18*, *45*−*48*) agree in general aspects of the expected mechanism. A general base is required to abstract the proton from C-5 of the uronic acid, generating an enolate anion intermediate, followed by proton donation by a general acid or water molecule and concomitant β-elimination of the leaving group. Proton abstraction and β-elimination are expected to proceed stepwise, as opposed to a concerted manner (*49*, *50*).

A significant challenge in effecting catalysis is the abstraction of the α-proton having a pK_a of 29−32 (*49*). This could be achieved by electrostatic interaction between a positively charged side chain forming a salt bridge to the carboxylate moiety or through binding of a metal cation (*10*, *50*). An alternative is electrophilic catalysis involving hydrogen bonding between some residue on the protein and the carboxyl moiety (*49*). Modeling of native lyase AC with CS^{tetra} shows that only Asn175 is able to form hydrogen bonds to the carboxylate moiety of GlcUA at the +1 subsite. This interaction is also observed in the lyase AC−DS^{hexa} complex, but not in the lyase AC−CS^{tetra} complex due to rotation of the GlcUA ring. Asparagine 175 is conserved throughout the bacterial hyaluronate lyases (Figure 6), and is equivalent to Asn349 in *S. pneumoniae* hyaluronate lyase (*14*) and Asn429 in group B *Streptococcal* hyaluronate lyase where its mutation to alanine abolishes activity (*16*). Hydrogen bonding interactions have also been proposed based on modeling hyaluronic acid in the active site of *S. pneumoniae* hyaluronate lyase (*14*). Unlike some polysaccharide lyases (*11*, *51*), no metal ion is present near the bound oligosaccharides in the models we describe here, eliminating this as a mode of electrostatic neutralization.

A feature of the lyase AC active site is the presence of a cluster of residues, His225, Tyr234, Arg288, and Glu371, that together form a catalytic tetrad (Figure 3c). The residues that constitute the tetrad are conserved between lyase AC and bacterial hyaluronate lyases (Figure 6). Three of the tetrad residues, His225, Tyr234, and Arg288 are likely to participate directly in catalysis, while the fourth, Glu371,

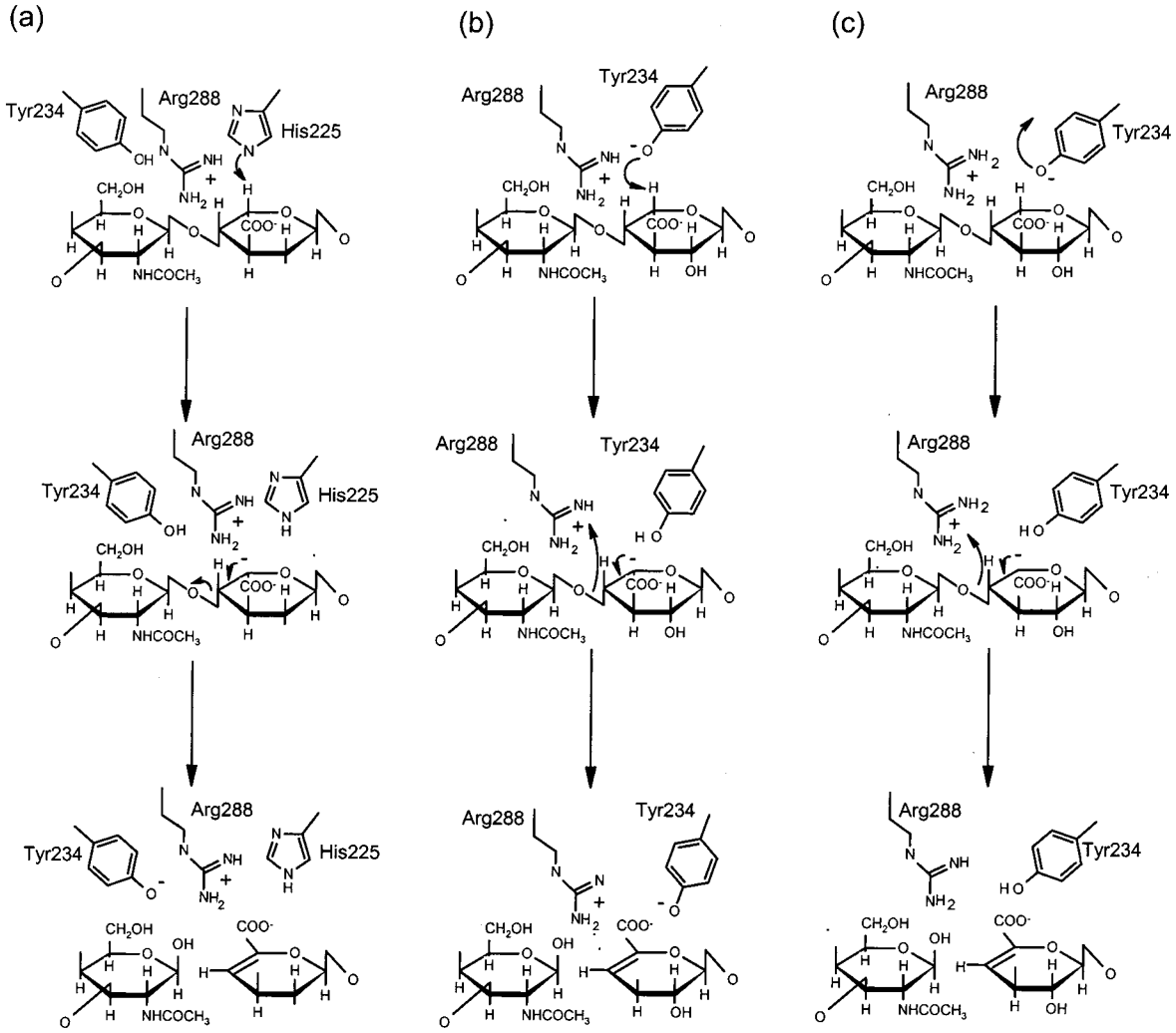

FIGURE 8: Possible roles of the lyase AC active site residues His225, Tyr234, and Arg288 in catalysis (a) His225 as general base and Tyr234 as general acid (b) Tyr234 as both general base and general acid and (c) Ty234 as general base, Arg288 as general acid. Descriptions of these three scenarios are given within the text.

may contribute to correctly position Arg288 and His225. This catalytic tetrad in some ways resembled that found in 3α-hydroxysteroid dehydrogenase, which consists of Asp 50, Tyr55, Lys84, and His117 (*52*). In the following, we consider three possible scenarios for the role of His225, Tyr234, and Arg288 in catalysis. Our present structural and mutagenesis data do not permit us to clearly discriminate between these three mechanisms at the present time.

(i) Scenario 1: His225 Acts as General Base, and Tyr234 as General Acid. This mechanism (Figure 8a) has been described for *S. pneumoniae* hyaluronate lyase (*14*, *15*) in which His399, corresponding to His225 of lyase AC, is predicted to be the general base. The homologous residue in Group B *Streptococcus* hyaluronate lyase, His479, when mutated to either Gly (*46*) or Ala (*16*) results in total loss of enzyme activity and has been suggested to function as the general base in this enzyme. In the crystal structure of lyase AC Tyr234Phe with CS^{tetra}, $NE2^{His225}$ is 4.3 Å from C-5 of GlcUA, a distance inconsistent with proton abstraction from the sugar. For His225 to function as the base, a shift of the oligosaccharide substrate in the binding site toward His225 would be required. The calculated pK_a of $NE2^{His225}$ at pH 7 for the free protein is 6.0, so this residue is expected to be in the deprotonated state at the pH optimum of the enzyme (*9*). While we observe a complete loss of activity with the His225Ala mutation, the corresponding His399Ala mutant of *S. pneumoniae* hyaluronate lyase retains 6% of the native enzyme activity, an unexpected result if this residue has a key function in catalysis. In this mechanistic proposal, Arg288 is suggested to play a role in charge neutralization of the enolate anion intermediate formed during catalysis.

In the mechanism proposed for hyaluronate lyase (*14*, *15*), Tyr408, the homologue of Tyr234 in lyase AC, has been postulated as the general acid. In the crystal structure of hyaluronate lyase with hyaluronan disaccharide, the distance of 2.8 Å between OH^{Tyr408} and O4 of the GlcNAc appears consistent with a role in proton donation. Our model indicates that OH^{Tyr234} is approximately 3.2 Å from the bridging oxygen atom. While this distance is longer than ideal for Tyr234 to act as the general acid, we cannot exclude this as a possibility. Mutagenesis of the homologous Tyr residue to Phe in *S. pneumoniae* (*14*) or group B *Streptococcal* (*16*) hyaluronate lyases totally abolished activity. We do not observe any water molecules close enough to the bridging oxygen that could act directly as proton donors.

(ii) Scenario 2: Tyr234 Acts as Both General Base and General Acid. One could speculate that Tyr234 acts to shuttle the proton in the reaction, first by abstracting it from C-5 of

GlcUA at the +1 subsite, thereby acting as a general base, then donating this same proton to the glycosidic oxygen atom of the leaving group, thereby acting as the general acid (Figure 8b). A similar mechanism, involving a histidine residue, has been proposed previously for hyaluronate lyase (*45*). A tyrosine acting as both general acid and base has been suggested in the reaction mechanism for 3α-hydroxysteroid dehydrogenase (*52*). On the basis of their proposal, interactions with either His117 or Lys84 facilitate functioning of Tyr55 as an acid, or base, respectively.

Preliminary modeling of lyase AC with CS^{tetra} indicates a distance of approximately 2.9 Å between OH^{Tyr234} and the C5(H) of GlcUA at the +1 subsite. This distance would suggest that Tyr234 is a reasonable candidate to act as the general base. Given, however, the broad pH optimum of lyase AC of between 6.8 and 8 (*9*), it is difficult to correlate lyase AC activity with Tyr234 as the general base unless its pK_a is significantly perturbed. If Tyr234 were to act as the base, it would have to be transiently deprotonated during catalysis. Another possibility for Tyr234 is that it participates in stabilization of the transition state as suggested for Tyr69 from *Bacillus circulans* xylanase (*53*). A precedent for a residue normally having a high pK_a acting as the general base has been suggested for Arg218 in the catalytic mechanism of pectate lyase C (*11*).

In the crystal structure of lyase AC Tyr234Phe bound to CS^{tetra}, the GlcUA located at the +1 subsite has rotated toward the Phe residue as a result of removal of the Tyr234 hydroxyl. This rotation has been accomplished through small alterations in the glycosidic bonds at either end of the sugar. When the native lyase AC and Tyr234Phe models are superposed, the +1 GlcUA of CS^{tetra} is now clearly too close to OH^{Tyr234}. This suggests that the hydrogen bond expected between $OH^{Tyr234}$and the +1 GlcUA, based on modeling, in addition to any possible catalytic function, plays an important role in precisely positioning this sugar in a catalytically competent state within the lyase AC active site.

(iii) Scenario 3: Tyr234 Acts as General Base, and Arg288 as General Acid. In structural terms, $NH2^{Arg288}$ is 2.7 Å from the bridging oxygen atom between the −1 and +1 subsites of the lyase ACTyr234Phe bound to CS^{tetra}, and would appear well situated to act as the general acid, donating a proton to the leaving group. Conversely, an active site Arg residue has been suggested to act as the general base in pectate lyase C (*11*). In lyase AC, Arg288 is precisely positioned through H-bonds with Glu371 and Glu376. Interactions with these residues would be expected to stabilize the positive charge of Arg288. A possible function for Arg288 is that it contributes to charge neutralization of the enolate anion intermediate during catalysis. Arginine 288 corresponds to Arg462 in *S. pneumoniae* hyaluronate lyase, and is present in the active site cleft of this enzyme, although it has not been implicated as a catalytic residue (*14*). Mutating the homologous residue, Arg542, in group B *Streptococcal* hyaluronate lyase decreases but does not abolish enzyme activity, raising questions about the precise function of this residue.

(iv) Role for Arg292 in Substrate Recognition, but Not Catalysis. Analysis of the lyase AC-oligosaccharide complexes and residual activity of the Arg292Ala mutant together provide a framework for understanding the role of this residue in the active site of AC lyase. All of the direct hydrogen bonding interactions between Arg292 and hyaluronic acid, dermatan sulfate or chondroitin sulfate are with either the *N*-acetyl or 4-sulfate groups of GalNAc or GlcNAc located at the −1 subsite. Therefore Arg292 has a specific role in the recognition of *N*-acetylated (hyaluronic acid; dermatan and chondroitin sulfates) or 4-*O*-sulfated hexoses (dermatan and chondroitin sulfates). As Arg292 is conserved in the family of bacterial hyaluronate lyases (Figure 6), it is expected to have the same function in these enzymes. Indeed, the homologous residue in *S. pneumoniae* hyaluronate lyase, Arg466, interacts with the *N*-acetyl group of the GlcNAc sugar from the disaccharide located toward the nonreducing end (*14*).

CONCLUSIONS

The lyase AC active site is located within a shallow tunnel formed by loops from the N- and C-terminal domains. Using a combination of crystallographic analysis of lyase AC-oligosaccharide complexes and mutagenesis of putative active site residues, we have identified His225, Tyr234, Arg288, and Glu371 as key active site residues. The catalytically inactive Tyr234Phe lyase AC mutant retains the ability to bind CS^{tetra}, suggesting a key function for this residue as either the general acid or general base in catalysis. The function of Arg292 appears primarily in recognition of the *N*-acetyl and 4-*O*-sulfo groups of GalNAc or GlcNAc. Additional mutagenesis, enzyme kinetic analysis and structural studies with transition state analogues will be required to precisely define the contributions of these residues to the catalytic mechanism of lyase AC.

ACKNOWLEDGMENT

We thank Robert Larocque for DNA constructs containing designed mutations, Daniel Dignard for DNA sequencing, Josée Plamandon for protein purification and Romas Kazlauskas for discussions on the catalytic mechanism. We also thank Ishan Capila for useful discussions on the mode of action of lyase AC. Traian Sulea is acknowledged for estimations of the pK_as of active site residues as well as energy calculations for isolated oligosaccharides. Thanks are extended to Leon Flaks of beamline X8C of the National Synchrotron Light Source for assistance in data collection.

REFERENCES

1. Jackson, R. L., Busch, S. J., and Cardin, A. D. (1991) *Physiol. Rev. 71*, 481−539.
2. Iozzo, R. V. (1998) *Annu. Rev. Biochem. 67*, 609−652.
3. Ernst, S., Langer, R., Cooney, C. L., and Sasisekharan, R. (1995) *Crit. Rev. Biochem. Mol. Biol. 30*, 387−444.
4. Sutherland, I. W. (1995) *FEMS Microbiol. Rev. 16*, 323−347.
5. Linhardt, R. J., Galliher, P. M., and Cooney, C. L. (1986) *Appl. Biochem. Biotechnol. 12*, 135−176.
6. See ref *3*.
7. Jandik, K. A., Gu, K., and Linhardt, R. J. (1994) *Glycobiology 4*, 289−296.
8. Baker, J. R., and Pritchard, D. G. (2000) *Biochem. J. 348* (Part 2), 465−471.
9. Gu, K., Linhardt, R. J., Laliberte, M., and Zimmermann, J. J. (1995) *Biochem. J. 312*, 569−577.
10. Gacesa, P. (1987) *FEBS Lett. 212*, 199−202.
11. Scavetta, R. D., Herron, S. R., Hotchkiss, A. T., Kita, N., Keen, N. T., Benen, J. A., Kester, H. C., Visser, J., and Jurnak, F. (1999) *Plant Cell 11*, 1081−1092.

12. Herron, S. R., Benen, J. A., Scavetta, R. D., Visser, J., and Jurnak, F. (2000) *Proc. Natl. Acad. Sci. U.S.A. 97*, 8762−8769.
13. Huang, W., Matte, A., Li, Y., Kim, Y. S., Linhardt, R. J., Su, H., and Cygler, M. (1999) *J. Mol. Biol. 294*, 1257−1269.
14. Li, S., Kelly, S. J., Lamani, E., Ferraroni, M., and Jedrzejas, M. J. (2000) *EMBO J. 19*, 1228−1240.
15. Ponnuraj, K., and Jedrzejas, M. J. (2000) *J Mol. Biol. 299*, 885−895.
16. Pritchard, D. G., Trent, J. O., Li, X., Zhang, P., Egan, M. L., and Baker, J. R. (2000) *Proteins 40*, 126−134.
17. Jenkins, J., Mayans, O., and Pickersgill, R. (1998) *J. Struct. Biol. 122*, 236−246.
18. Féthière, J., Eggimann, B., and Cygler, M. (1999) *J. Mol. Biol. 288*, 635−647.
19. Yoon, H. J., Mikami, B., Hashimoto, W., and Murata, K. (1999) *J. Mol. Biol. 290*, 505−514.
20. Hiyama, K., and Okada, S. (1976) *J. Biochem. (Tokyo) 80*, 1201−1207.
21. Gu, K., Liu, J., Pervin, A., and Linhardt, R. J. (1993) *Carbohydr. Res. 244*, 369−377.
22. Pervin, A., al Hakim, A., and Linhardt, R. J. (1994) *Anal. Biochem. 221*, 182−188.
23. Tkalec, A. L., Fink, D., Blain, F., Zhang-Sun, G., Laliberte, M., Bennett, D. C., Gu, K., Zimmermann, J. J., and Su, H. (2000) *Appl. Environ. Microbiol. 66*, 29−35.
24. Vieira, J., and Messing, J. (1991) *Gene 100*, 189−194.
25. Su, H., Shao, Z., Tkalec, A. L., Blain, F., and Zimmermann, J. J. (2001) *Microbiology* (in press).
26. Zimmermann, J. J., Langer, R., and Cooney, C. L. (1990) *Appl. Environ. Microbiol. 56*, 3593−3594.
27. Féthière, J., Shilton, B. H., Li, Y., Allaire, M., Laliberte, M., Eggimann, B., and Cygler, M. (1998) *Acta Crystallogr., Sect. D 54*, 279−280.
28. Otwinowski, Z., and Minor, W. (1997) *Methods Enzymol. 276*, 307−326.
29. Jones, T. A., Zhou, J. Y., Cowan, S. W., and Kjeldgaard, M. (1991) *Acta Crystallogr., Sect. A 47*, 110−119.
30. Brünger, A. T., Adams, P. D., Clore, G. M., DeLano, W. L., Gros, P., Grosse-Kunstleve, R. W., Jiang, J. S., Kuszewski, J., Nilges, M., Pannu, N. S., Read, R. J., Rice, L. M., Simonson, T., and Warren, G. L. (1998) *Acta Crystallogr., Sect. D 54*, 905−921.
31. Laskowski, R. A., MacArthur, M. W., Moss, D. S., and Thornton, J. M. (1993) *J. Appl. Crystallogr. 26*, 283−291.
32. Murzin, A. G., Brenner, S. E., Hubbard, T., and Chothia, C. (1995) *J. Mol. Biol. 247*, 536−540.
33. Mitra, A. K., Arnott, S., Atkins, E. D., and Isaac, D. H. (1983) *J. Mol. Biol. 169*, 873−901.
34. Scott, J. E., Heatley, F., and Wood, B. (1995) *Biochemistry 34*, 15467−15474.
35. Davies, G. J., Wilson, K. S., and Henrissat, B. (1997) *Biochem. J. 321* (Part 2), 557−559.
36. Hileman, R. E., Fromm, J. R., Weiler, J. M., and Linhardt, R. J. (1998) *Bioessays 20*, 156−167.
37. Nagy, T., Simpson, P., Williamson, M. P., Hazlewood, G. P., Gilbert, H. J., and Orosz, L. (1998) *FEBS Lett. 429*, 312−316.
38. Ponyi, T., Szabo, L., Nagy, T., Orosz, L., Simpson, P. J., Williamson, M. P., and Gilbert, H. J. (2000) *Biochemistry 39*, 985−991.
39. Teeri, T. T., Koivula, A., Linder, M., Wohlfahrt, G., Divne, C., and Jones, T. A. (1998) *Biochem. Soc. Trans. 26*, 173−178.
40. Parsiegla, G., Reverbel-Leroy, C., Tardif, C., Belaich, J. P., Driguez, H., and Haser, R. (2000) *Biochemistry 39*, 11238−11246.
41. Schmidt, A., Gübitz, G. M., and Kratky, C. (1999) *Biochemistry 38*, 2403−2412.
42. Varrot, A., Schulein, M., and Davies, G. J. (1999) *Biochemistry 38*, 8884−8891.
43. Zou, J., Kleywegt, G. J., Stahlberg, J., Driguez, H., Nerinckx, W., Claeyssens, M., Koivula, A., Teeri, T. T., and Jones, T. A. (1999) *Struct. Folding Des. 7*, 1035−1045.
44. Parsiegla, G., Juy, M., Reverbel-Leroy, C., Tardif, C., Belaich, J. P., Driguez, H., and Haser, R. (1998) *EMBO J. 17*, 5551−5562.
45. Greiling, H., Stuhlsatz, H. W., Eberhard, T., and Eberhard, A. (1975) *Connect. Tissue Res. 3*, 135−139.
46. Lin, B., Averett, W. F., and Pritchard, D. G. (1997) *Biochem. Biophys. Res. Commun. 231*, 379−382.
47. Sasisekharan, R., Leckband, D., Godavarti, R., Venkataraman, G., Cooney, C. L., and Langer, R. (1995) *Biochemistry 34*, 14441−14448.
48. Shriver, Z., Hu, Y., Pojasek, K., and Sasisekharan, R. (1998) *J. Biol. Chem. 273*, 22904−22912.
49. Gerlt, J. A., and Gassman, P. G. (1992) *J. Am. Chem. Soc. 114*, 5928−5934.
50. Guthrie, J. P., and Kluger, R. (1993) *J. Am. Chem. Soc. 115*, 11569−11572.
51. Liu, D., Shriver, Z., Godavarti, R., Venkataraman, G., and Sasisekharan, R. (1999) *J. Biol. Chem. 274*, 4089−4095.
52. Schlegel, B. P., Jez, J. M., and Penning, T. M. (1998) *Biochemistry 37*, 3538−3548.
53. Sidhu, G., Withers, S. G., Nguyen, N. T., McIntosh, L. P., Ziser, L., and Brayer, G. D. (1999) *Biochemistry 38*, 5346−5354.
54. Guex, N., and Peitsch, M. C. (1997) *Electrophoresis 18*, 2714−2723.
55. Nicholls, A., Sharp, K. A., and Honig, B. (1991) *Proteins: Struct., Funct., Genet. 11*, 281−296.
56. Wallace, A. C., Laskowski, R. A., and Thornton, J. M. (1995) *Protein Eng. 8*, 127−134.
57. Thompson, J. D., Higgins, D. G., and Gibson, T. J. (1994) *Nucleic Acids. Res. 22*, 4673−4680.

BI0024254